Journal of Southeast University (English Edition) Vol. 24, No. 2, pp. 234 – 237 June 2008 ISSN 1003—7985

Multi-branched carbazole derivatives for two-photon absorption and two-photon excited fluorescence

Qian Ying[1] Huang Wei[2] Lu Zhifeng[1] Meng Kang[1] Lü Changgui[2] Cui Yiping[2]

([1]School of Chemistry and Chemical Engineering, Southeast University, Nanjing 211189, China)

([2]School of Electronic Science and Engineering, Southeast University, Nanjing 210096, China)

Abstract: Carbazole-core multi-branched chromophores 9-ethyl-3, 6-bis(2-{4-[5-(4-tert-butyl-phenyl)-[1, 3, 4] oxadiazol-2-yl]-phenyl}-vinyl)-carbazole(3) and 9-ethyl-3-(2-{4-[5-(4-tert-butyl-phenyl)-[1, 3, 4] oxadiazol-2-yl]-phenyl}-vinyl)-carbazole (2) are synthesized through Wittig reaction and characterized by nuclear magnetic resonance (NMR) and infrared (IR). The two-photon absorption properties of chromophores are investigated. These chromophores exhibit large two-photon absorption cross-sections and strong blue two-photon excited fluorescence. The cooperative enhancement of two-photon absorption (TPA) in the multi-branched structures is observed. This enhancement is partly attributed to the electronic coupling between the branches. The electronic push-pull structures in the arm and their cooperative effects help the extended charge transfer for TPA.

Key words: two-photon absorption; two-photon excited fluorescence; multi-branched chromophores; carbazole derivatives

Organic multibranched systems are utilized for two-photon absorption (TPA) effects which may have applications in optical power limiting, two-photon fluorescence imaging, three-dimensional optical data storage, frequency-up-converted lasing and two-photon photodynamic therapy[1-3]. A major advantage of the multi-branched structure originates from the intramolecular coupling and cooperative enhancement of TPA. This enhancement is correlated with intramolecular interactions that occur between the branches and the centers of the molecules. Increasing the extent of charge transfer from the ends to the middle results in a large increase of two-photon absorption cross-section values[4-9].

In this paper, we design and synthesize the multibranched carbazole-core chromophores. The molecular structures of chromophores 1, 2, and 3 are presented in Fig. 1. The fundamental building block molecule is a 2-(4-tert-butylphenyl)-5-(4-vinylphenyl)-[1, 3, 4] oxadiazole (chromophore 1), which can be considered as a repeat unit for the larger chromophores 2 and 3. We report two-photon absorption and two-photon excited fluorescence of multibranched chromophores 9-ethyl-3, 6-bis(2-{4-[5-(4-tert-butylphenyl)-[1, 3, 4] oxadiazol-2-yl]-phenyl}-vinyl)-carbazole (chromophore 3) and 9-ethyl-3-(2-{4-[5-(4-tert-butyl-phenyl)-[1, 3, 4] oxadiazol-2-yl]-phenyl}-vinyl)-carbazole (chromophore 2). Both compounds involve linkage of one- or two-chromophore units through conjugated groups. The terminal acceptor group is a substituted [1, 3, 4] oxadiazol group, and the center of the molecules is an electron-donor carbazole segment. Compared with one-dimensional molecules, multi-branched chromophores have appeared to show promising properties. A butyl moiety is attached to the end of each arm to induce optical transparency as well as good solubility to various organic solvents.

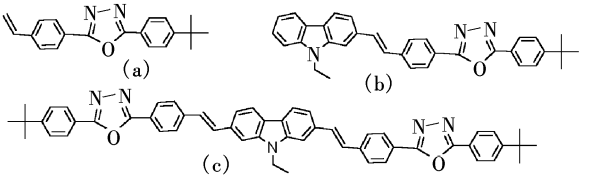

Fig. 1 Chemical structures of chromophores. (a) Chromophore 1; (b) Chromophore 2; (c) Chromophore 3

1 Experimental

1.1 Chemicals and measurements

All the optical characterizations were conducted using solutions of compounds in 1, 2-dichloromethane. ^{1}H-NMR measurements were determined with a Brucker 500 MHz apparatus, with TMS (tetramethyl silane) as internal standard and $CDCl_3$ (deuterated chloroform) as solvent. FT-IR spectra were recorded on a Nicolet 750 series in the region of 4 000 to 400 cm^{-1} using KBr pellets. UV-visible absorption was conducted using a Shimadzu UV-3600 spectrophotometer. Single-photon fluorescence was conducted using an Edinbough F900 spectrofluorophotometer.

Two-photon absorption cross-section values of all the chromophores in solution were investigated by a direct nonlinear transmission (NLT) method with nanosecond pulse[10-11]. This method involves the measurement and study of the relationship between optical input and output intensities. Basically, a linearly polarized 800 nm pulsed laser beam is used as the testing beam, which is provided by a dye laser system pumped with a frequency-doubled and Q-switched Nd: YAG laser. This laser beam is focused and passed through a quartz cuvette filled with the sample solution and the transmitted laser beam from the sample cell can be detected by an optical power meter. Thus, if the tested sample does not have a linear absorption at 800 nm, only the transmissivity change due to pure nonlinear absorption can be measured. The experimental setup and data processing procedures are basically the same as those described in previous publications.

1.2 Synthesis and characterizations

The synthesis of electron-acceptor functionalized oxadiazole compound was accomplished by a straightforward series of reactions. As shown in Fig. 2, before the formation of a heterocyclic oxadiazole ring, the coupling reaction between 4-methyl benzoyl chloride and 4-tert-butyl benzoic acid hydra-

Received 2007-06-25.

Biography: Qian Ying (1969—), female, doctor, professor, yingqian@seu.edu.cn.

Foundation items: The National Natural Science Foundation of China (No. 60678042), the Natural Science Foundation of Jiangsu Province (No. BK2006553), the Pre-Research Project of the National Natural Science Foundation supported by Southeast University (No. 9207041399).

Citation: Qian Ying, Huang Wei, Lu Zhifeng, et al. Multi-branched carbazole derivatives for two-photon absorption and two-photon excited fluorescence[J]. Journal of Southeast University (English Edition), 2008, 24 (2): 234 – 237.

zide should be accomplished first. Simple ring formation by condensation of water from amide compound M_2 in the presence of $POCl_3$ gives rise to compound M_3. Free radical bromination of M_3 is set-up to afford bromomethyl compound M_4 and to be transformed into phosphonium bromide salt M_5. Finally, this Wittig precursor, M_5, is reacted with corresponding aldehydes to give the target chromophores 1, 2 and 3.

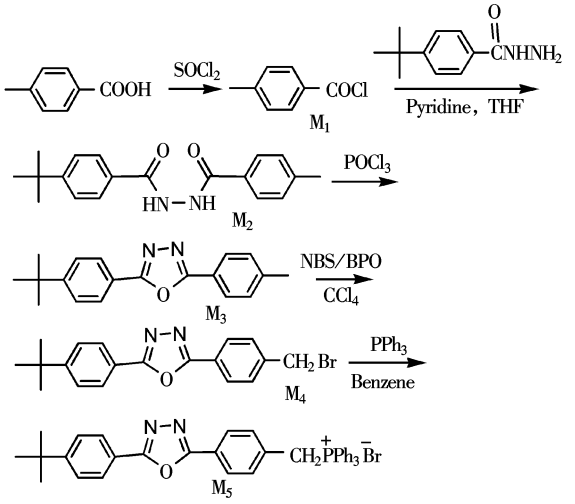

Fig. 2 Synthetic routes of compounds M_1 to M_5

Wittig reaction is an important synthetic route for the formation of an olefin functional group. In general, Wittig reaction involves the coupling between an aldehyde and a phosphorus ylide to produce a carbon-carbon double bond. Benzaldehyde derivatives and benzylphosphonium bromide salt are used as the reactants in Fig. 3. Relatively low yields of chromophores 1, 2 and 3 were obtained (about 60% to 70%) after carefully being purified by column chromatography and several runs of recrystallization. It is noteworthy that in our case, the major product of Wittig reaction is the "trans" form of the stilbenoid compounds. All the chromophores after thorough purification are highly soluble in many organic solvents.

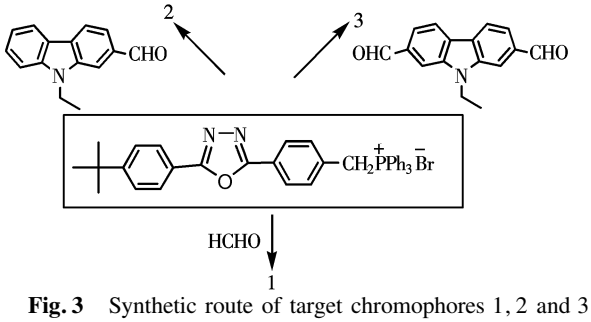

Fig. 3 Synthetic route of target chromophores 1, 2 and 3

● 2-(4-tert-butylphenyl)-5-(4-vinylphenyl)-[1, 3, 4] oxadiazole (1)

^{1}HNMR (500 MHz, $CDCl_3$): δ 1.39 (s, 9H, CH_3), 5.41 (d, 1H, J = 10.85, $=CH_2$), 5.89 (d, 1H, J = 17.60, $=CH_2$), 6.77 to 6.82 (m, 1H, —CH =), 7.57 to 7.59 (m, 4H, ph-H), 8.08 to 8.18 (m, 4H, ph-H). IR: γ (cm^{-1}) 2 956, 2 865 (—CH_3), 2 902 (—CH_2—), 1 616 (—CH =CH—), 3 062, 1 097 (oxadiazole ring), 1 590, 1 494 (benzene ring).

● 9-ethyl-3-(2-{4-[5-(4-tert-butylphenyl)-[1, 3, 4] oxadiazol-2-yl]-phenyl}-vinyl)-carbazole (2)

^{1}HNMR (500 MHz, $CDCl_3$): δ 1.38 (s, 9H), 1.45 (t, 3H, J = 4.00 Hz), 4.38 to 4.41 (m, 2H), 7.19 (d, 1H, J = 12.00 Hz), 7.21 (d, 1H, J = 12.00 Hz), 7.38 to 7.44 (m, 4H), 7.47 (d, 2H, J = 8.00 Hz), 7.55 (d, 2H, J = 8.50 Hz), 7.70 (d, 2H, J = 8.50 Hz), 8.05 (d, 2H, J = 8.00 Hz), 8.13 (d, 2H, J = 7.50 Hz), 8.28 (s, 1H). IR: γ (cm^{-1}) 2 960, 2 864 (—CH_3), 2 902 (—CH_2—), 1 602 (—CH =CH—), 3 042, 1 095 (oxadiazole ring), 1 594, 1 486 (benzene ring).

● 9-ethyl-3, 6-bis(2-{4-[5-(4-tert-butylphenyl)-[1, 3, 4] oxadiazol-2-yl]-phenyl}-vinyl)-carbazole (3)

^{1}HNMR (500 MHz, $CDCl_3$): δ 1.40 (s, 18H), 1.49 (t, 3H, J = 4.00 Hz), 4.38 to 4.41 (m, 2H), 6.66 (d, 2H, J = 12.00 Hz), 6.94 (d, 2H, J = 12.00 Hz), 7.44 to 7.49 (m, 6H), 7.51 (d, 2H, J = 8.50 Hz), 7.54 (d, 2H, J = 7.00 Hz), 7.59 (d, 2H, J = 8.50 Hz), 7.70 (d, 2H, J = 7.50 Hz), 7.75 (d, 2H, J = 7.50 Hz), 8.10 (d, 2H, J = 8.00 Hz), 8.12 (d, 2H, J = 8.00 Hz), 8.18 (d, 2H, J = 7.50 Hz). IR: γ (cm^{-1}) 2 964, 2 867 (—CH_3), 2 902 (—CH_2—), 1 612 (—CH =CH—), 3 054, 1 097 (oxadiazole ring), 1 592, 1 492 (benzene ring).

2 Results and Discussion

2.1 Linear optical properties of chromophores

It is noted that there is no absorption in the range from 450 to 1 000 nm for chromophores 1, 2 and 3. The maximum peaks of linear absorption corresponding to the charge-transfer bands are at 357 nm for the single branched compound 2 and at 391nm for the bi-branched compound 3 in CH_2Cl_2 (the maximum absorption band of compound 1 observed at 305 nm). The maximum molar extinction coefficients of the two chromophores in CH_2Cl_2 are 0.32×10^5 and 0.95×10^5 L/(cm · mol) for 2 and 3, respectively. Chromophores 2 and 3 fluoresce blue in the solid state under the conventional laboratory UV-lamp. Using a 400 nm excitation wavelength in CH_2Cl_2 at a concentration of 0.1 mmol/L, Fig. 4 (a) shows that the single-photon excited fluorescence of 3 is in the blue region with a peak at 475 nm. Chromophore 2 exhibits a

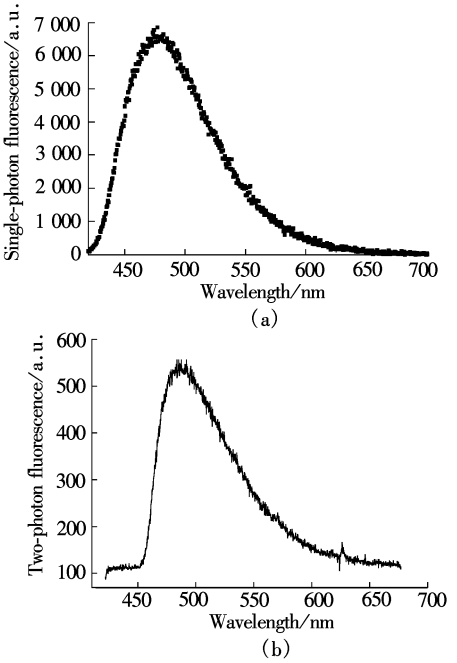

Fig. 4 Fluorescence of chromophore 3 in CH_2Cl_2. (a) Single-photon excited fluorescence (SPEF) (0.1 mmol/L); (b) Two-photon excited fluorescence (TPEF) (10 mmol/L)

strong emission in the blue region with a peak at 468 nm. The two compounds have short fluorescence lifetimes of about 2 ns.

2.2 Two-photon excited fluorescence properties of chromophores

The very strong frequency-upconverted fluorescence emissions can be observed from chromophore 2 and 3 solutions excited with a Nd: YAG pumped dye laser(Continuum PR Ⅱ 8010) at the wavelength 800 nm in CH_2Cl_2 at a concentration of 10^{-2} mol/L. Fig. 4(b) shows that the maximum peak of two-photon excited fluorescence for chromophore 3 is at 486 nm, and the blue fluorescence is obtained. That is, the same trend is observed in the single-photon and two-photon emission spectra of compounds as one increases the content of the chromophore moiety per molecule. This is a clear indication of some interactions between chromophore moieties in the molecules, resulting in charge redistribution and extended delocalization. The red-shift for two-photon fluorescence, in comparison with the corresponding single-photon fluorescence, can be explained by re-absorption.

2.3 Two-photon absorption cross-sections

The TPA cross-section values of compounds are investigated with an IR dye laser pumped by a Q-switched and frequency-double Nd: YAG laser by a direct nonlinear transmission(NLT) method. The nonlinear transmission technique involves measuring the transmitted intensity over incident light intensity. It is seen that the intensity of the transmitted laser beam I increased nonlinearly as that of the incident laser beam I_0 increased. The nonlinear absorption coefficient is obtained by fitting the experimental data with the following equation[12-14]

$$I = \frac{I_0}{1 + I_0 L\beta} \tag{1}$$

where L is the thickness of the sample and β is the nonlinear absorption coefficient which is related to the effective TPA molecular cross section as

$$\sigma_2 = \frac{h\nu\beta}{N_0} \tag{2}$$

where N_0 is the molecular density in the ground state, $h\nu$ is the energy of the incident photon, and σ_2 is in units of cm^4s. Although using this σ_2 value provides some agreement with the data in the low-energy regime where the NLT begins to roll over, for the most part it leads to an overestimation of the nonlinear loss for higher pulse energies[15].

The obtained TPA cross-sections of chromophores 1 and 3 from 575 to 900 nm at intervals of 25 nm are shown in Fig. 5. Obviously, the TPA cross-sections of 2 and 3 are higher than those of 1 at every wavelength. The maximum values are measured in 725 nm to be 3.98×10^{-46} ($cm^4 \cdot s$)/photon for chromophore 3, 1.35×10^{-46} ($cm^4 \cdot s$)/photon for chromophore 2, and 0.35×10^{-46} ($cm^4 \cdot s$)/photon for chromophore 1, respectively. Experiments clearly indicate a relative increase in the effective nonlinear absorption cross-section as the number of chromophore moieties increases, which is not linear.

The two-photon absorption cross-section is related to the imaginary part of molecular third-order nonlinear polarizability. It is reasonable to limit a sum-over-states expansion to three closest energy levels(three-level model), namely, the ground state(index 0), the two-photon excited state f, and a main intermediate electronic state i, then the peak cross section can be expressed as [16-18]

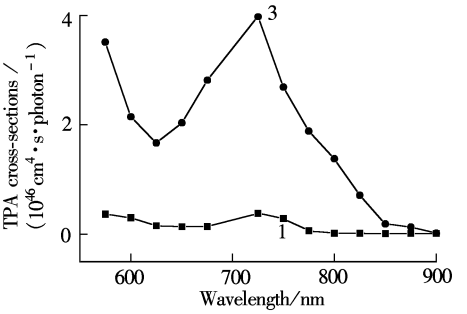

Fig. 5 TPA cross-sections of chromophores 1 and 3 from 575 to 900 nm in CH_2Cl_2

$$\sigma_2 \propto \frac{(E_{f0}/2)^2 M_{i0}^2 M_{fi}^2}{(E_{i0} - E_{f0}/2)^2 \Gamma_{f0}} \tag{3}$$

where Γ_{f0} is the linewidth of the two-photon transition; E_{nm} and M_{nm} are the energy difference and the transition dipole moment between the states n and m, respectively.

A number of factors influence the TPA magnitude, among which are electronic delocalization and intramolecular charge-transfer phenomena. This enhancement in σ_2 is correlated to an intramolecular charge redistribution that occurs between the ends and the center of the molecules. Increasing the conjugation length of the molecule or increasing the extent of multibranched charge from the ends to the middle results in a large increase in σ_2. It is found that the increase in chromophore density is an important factor which governs the magnitude of the cross sections of these molecules. The electronic push-pull structures in the arm and their cooperative effect help the extended charge transfer for TPA.

2.4 Optical power limiting

Optical power limiting is an area of growing interest owing to applications such as eye and photodetector protection against intense tunable laser pulses. An ideal optical limiter is perfectly transparent at low intensities below a predetermined critical intensity level, above which the transmitted intensity remains at a constant value. The principle of optical power limiting effects is based on the fact that a large input signal change will only lead to a small output change. Fig. 6 shows the optical power limiting behavior of the chromophore 3 measured by the NLT method. The basic parameters of this dye laser output are at an 800 nm wavelength, 8 ns pulse width, and 1 to 2 mJ pulse energy. In Fig. 6, one can easily find that at a high input level, a larger input intensity variation will result in much smaller output intensity variation due to the intrinsic TPA property. The most interesting feature of Fig. 6 is that the output/input curve levels off when the input intensity increases from 0.5 to 3.5 GW/cm^2. This type of output/input characteristic curve can be used for optical peak power limiting and stabilization, which means that a larger input peak power fluctuation will become a much smaller output fluctuation after passing through the nonlinear absorptive chromophores with a large TPA value. The optical limiting ability is in the order of chromophore 3 > chromophore 2 > chromophore 1.

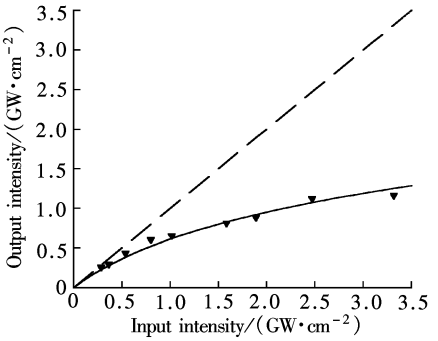

Fig. 6 The nonlinear transmission intensity vs. the input intensity for chromophore 3

3 Conclusion

As a result, multibranched chromophores 2 and 3 show larger TPA cross-sections at every wavelength than the single oxadiazole chromophopre 1. The optical limiting ability is in the order of chromophore 3 > chromophore 2 > chromophore 1. The cooperative enhancement of TPA in the multi-branched structures is observed. This enhancement is partly attributed to the electronic coupling between the branches. The electronic push-pull structures in the arm and their cooperative effect help the extended charge transfer for TPA.

References

[1] Chung S J, Lin T C, Kim K S, et al. Two-photon absorption and excited-state energy-transfer properties of a new multibranched molecule[J]. *Chem Mater*, 2001, **13**(11): 4071 − 4076.

[2] Kato S, Matsumoto T, Shigeiwa M, et al. Novel 2, 1, 3-benzothiadiazole-based red-fluorescent dyes with enhanced two-photon absorption cross-sections[J]. *Chem Eur J*, 2006, **12**(8): 2303 − 2317.

[3] Bhaskar A, Ramakrishna G, Haley M M, et al. Building symmetric two-dimensional two-photon materials[J]. *J Am Chem Soc*, 2006, **128**(43): 13972 − 13973.

[4] Huang P, Shen J, Pu S, et al. Synthesis and characterization of new fluorescent two-photon absorption chromophores[J]. *J Mater Chem*, 2006, **16**(9): 850 − 857.

[5] Yang W J, Kim D Y, Kim C H, et al. Triphenylamine derivatives with large two-photon cross-sections[J]. *Org Lett*, 2004, **6**(9): 1389 − 1392.

[6] Wang Y, He G S, Prasad P N, et al. Ultrafast dynamics in multibranched structures with enhanced two-photon absorption[J]. *J Am Chem Soc*, 2005, **127**(29): 10128 − 10129.

[7] Zheng Q, He G S, Baev A, et al. Experimental and quantum chemical studies of cooperative enhancement of three-photon absorption, optical limiting, and stabilization behaviors in multibranched and dendritic structures[J]. *J Phys Chem B*, 2006, **110**(30): 14604 − 14610.

[8] Zheng Q, He G S, Prasad P N. π-conjugated dendritic nanosized chromophore with enhanced two-photon absorption[J]. *Chem Mater*, 2005, **17**(24): 6004 − 6011.

[9] Chung S J, Kim K S, Lin T C, et al. Cooperative enhancement of two-photon absorption in multi-branched structures[J]. *J Phys Chem B*, 1999, **103**(49): 10741 − 10745.

[10] Lee H J, Sohn J, Hwang J, et al. Triphenylamine-cored bifunctional organic molecules for two-photon absorption and photorefraction[J]. *Chem Mater*, 2004, **16**(3): 456 − 465.

[11] He G S, Lin T, Cui Y P, et al. Two-photon excited intramolecular energy transfer and light-harvesting effect in novel dendritic systems[J]. *Opt Lett*, 2003, **28**(10): 768 − 770.

[12] Lei H, Huang Z L, Wang H Z, et al. Two-photon absorption spectra of new organic compounds[J]. *Chem Phys Lett*, 2002, **352**(2): 240 − 244.

[13] He G S, Xu G C, Prasad P N, et al. Two-photon absorption and optical-limiting properties of novel organic compounds[J]. *Opt Lett*, 1995, **20**(5): 435 − 437.

[14] He G S, Bhawalker J D, Zhao C F, et al. Optical limiting effect in a two-photon absorption dye doped solid matrix[J]. *Appl Phys Let*, 1995, **67**(17): 2433 − 2435.

[15] Sutherland R, Brant M C, Heinrichs J, et al. Excited-state characterization and effective three-photon absorption model of two-photon-induced excited-state absorption in organic push-pull charge-transfer chromophores[J]. *J Opt Soc Am B*, 2005, **22**(9): 1939 − 1948.

[16] Drobizhev M, Rebane A, Suo Z, et al. One-, two- and three-photon spectroscopy of conjugated dendrimers: cooperative enhancement and coherent domains[J]. *Journal of Luminescence*, 2005, **111**(2): 291 − 305.

[17] Slepkov A D, Hegmann F A, Tykwinski R R, et al. Two-photon absorption in two-dimensional conjugated quadrupolar chromophores[J]. *Opt Lett*, 2006, **31**(22): 3315 − 3317.

[18] Rumi M, Ehrlich J E, Heikal A A, et al. Structure-property relationships for two-photon absorbing chromophores: bis-donor diphenylpolyene and bis(styryl) benzene derivatives[J]. *J Am Chem Soc*, 2000, **122**(39): 9500 − 9510.

多分枝咔唑衍生物的双光子吸收和双光子荧光性质

钱 鹰[1] 黄 维[2] 路志锋[1] 孟 康[1] 吕昌贵[2] 崔一平[2]

([1] 东南大学化学化工学院,南京 211189)

([2] 东南大学电子科学与工程学院,南京 210096)

摘要: 通过 Wittig 反应合成了咔唑衍生物 9-乙基-3-{5-(4-叔丁基苯基)-[1,3,4] 二唑-2-苯乙烯基}-咔唑(2)和 9-乙基-3,6-双{5-(4-叔丁基苯基)-[1,3,4] 噁二唑-2-苯乙烯基}-咔唑(3),用核磁共振和红外光谱进行了结构表征. 实验测定了咔唑衍生物的双光子吸收和双光子诱导荧光性质. 这些化合物的双光子吸收截面较大,在 800 nm 波长的激光激发下发出很强的蓝色双光子上转换荧光. 实验中观察到了多枝结构在双光子吸收中的协同效应. 这样的协同效应部分原因是由于多分枝间电子耦合作用,多分枝分子中重复单元的推拉电子结构和协同效应有效地增强了分子的双光子吸收性质.

关键词: 双光子吸收;双光子诱导荧光;多分枝分子;咔唑衍生物

中图分类号: O626.24